

**ARTICLE**

# Growth and Invasion of 3D Spheroid Tumor of HeLa and CasKi Cervical Cancer Cells

Kalaivani Muniandy<sup>1</sup>, Zuhaida Asra Ahmad<sup>1,4</sup>, Sylvia Annabel Dass<sup>1</sup>, Shaharum Shamsuddin<sup>2</sup>, Nethia Mohana Kumaran<sup>3</sup> and Venugopal Balakrishnan<sup>1,\*</sup>

<sup>1</sup>Institute for Research in Molecular Medicine, Universiti Sains Malaysia, Pulau Pinang, 11800, Malaysia

<sup>2</sup>School of Health Sciences, Universiti Sains Malaysia, Health Campus, Kelantan, 16150, Malaysia

<sup>3</sup>School of Biological Sciences, Universiti Sains Malaysia, Pulau Pinang, 11800, Malaysia

<sup>4</sup>Institute for Clinical Research (ICR), National Institute of Health (NIH), Sekekyen U13, Bandar Setia Alam, Shah Alam, 41070, Selangor, Malaysia

\*Corresponding Author: Venugopal Balakrishnan. Email: venugopal@usm.my

Received: 27 January 2021 Accepted: 20 May 2021

**ABSTRACT**

Spheroids are generally self-assembled cells with the ability to generate their extracellular matrix, including the complex cell-matrix and the cell-cell interactions that resemble the functional characteristics of the corresponding tissue *in vivo*. The study aimed to develop a three-dimensional (3D) spheroid system for the cervical cancer cell lines, HeLa (HPV18), CaSki (HPV16), SiHa (HPV16), C33A (non-HPV), HT3 (non-HPV) as well as to identify its biological activity in the extracellular form. For the formation of the cervical cancer spheroids, the liquid overlay approach was applied, followed by embedding to the bovine collagen I matrix. Spheroid formation using the liquid overlay approach is achieved by growing the cells on a non-adhesive surface to prevent cellular adhesion, resulting in the cells forming aggregates and, subsequently, the spheroids. The obtained data shows the definite biological behavior of each of the particular cervical cancer cell lines, indicating that cells adapt their natural phenotype in a three-dimensional microenvironment.

**KEYWORDS**

3D spheroid system; HeLa; CaSki; SiHa; C33A; HT3

## 1 Introduction

Cervical carcinoma is one of the most common gynecologic malignancies and is known to be one of the root causes of cancer death in females globally [1]. According to the Global Cancer Observatory (GLOBOCON) report, cervical cancer accounted for 6.8% of the total cancer cases in Malaysia in 2020, with an estimated death rate of 3.4% [2]. The Malaysian National Cancer Registry (MNCR) concluded cervical cancer malignancy to be the third most prevalent cancer amongst females after breast and colorectal cancer and the seventh most common cancer in the whole human population [3].

Epidemiologic studies have shown that sexually transmitted human papillomavirus (HPV) is strongly associated with cervical cancer, independent of other risk factors [4]. The majority of oncogenic or high-risk (HR) forms correlated with invasive cervical cancer malignancy are primarily contributed by either



the *Human papillomavirus 16* (alpha-9) or *Human papillomavirus 18* (alpha-7) species groups, which accounts for 75% and 15% of all cervical cancers worldwide, respectively [1]. The HPV viruses, which play crucial contributing factors to cervical cancer malignancy are transmitted sexually in human [5].

Cancer biology research has a significant relation to the established cell lines. The traditional cell culture model has been a platform for the drug discovery, cell signaling, gene expression, and cytotoxicity evaluation of the compound [6]. It poses a straightforward, rapid, as well as cost-effective approach to minimize large-scale and cost-intensive animal screening. In the two-dimensional (2D) cell culture model, cell propagation is easily achieved and maintained under well-defined experimental conditions, which are highly reproducible. However, the primary limitation of the two-dimensional cell culture model is that the cells are grown in a varying environment from their native tumor microenvironment [7].

Although additional elements such as fetal bovine serum (FBS) as well as various other sources of nourishment may provide the essential growth factors to replicate the extracellular matrix (ECM), the framework of the stroma is still not successfully resembled in the 2D model [8]. Initial findings suggested that the growth of epithelial cells within the ECM may likely contribute significant effects to their phenotype, metabolism, and cell signaling state compared to the traditional 2D cell culture using plastic medium [9]. In contrast, the three-dimensional (3D) culture systems offer efficient *in vitro* platforms by mimicking the *in vivo* environment, making it possible to investigate the cellular responses in a setting resembling the actual tumor [10]. Thus, in this study, we intended to establish a three-dimensional (3D) cell culture model from the HeLa, Ca Ski, SiHa C33-A, and HT3 cervical cancer cells and determine the biological behavior of the cells in the collagen matrix.

## 2 Materials and Methods

### 2.1 Two-Dimensional Cell Culture

The human cervical cancer cell lines HeLa (ATCC® CCL2™), Ca Ski (ATCC® CRL-1550™) C-33 A [c-33a] ATCC® HTB-31™) were obtained from American Type Culture Collection (Manassa, USA). SiHa, C33-A, C33-A E7, C33-A pcDNA, and HT3 cell lines were provided by Associate Professor Dr. Nikolas Haass (University of Queensland, Australia). HeLa, SiHa C-33A, C33-A E7, C33A pcDNA, and HT3 cells were cultured in the Dulbecco's Modified Eagle Medium (Gibco), and the CaSki cells were cultured in the Roswell Park Memorial Institute Medium-1640 (Gibco). All media were supplemented with 10% fetal bovine serum. The cells were maintained at 37°C in a humidified incubator containing 5% CO<sub>2</sub>.

### 2.2 Generation of Spheroids

Cervical cancer spheroids were produced based on the liquid overlay method [11,12]. Firstly, 1.5% of (w/v) agar was prepared by dissolving the agarose powder (Sigma-Aldrich) in 1X PBS and microwaved for two minutes until the agar powder was fully dissolved. Instantly 0.1 ml of the molten agar solution was dispensed into a 96-well flat-bottom plate via a multichannel pipette. The agar plate was then left at room temperature to solidify. Then, 0.2 ml of complete media containing 5000 cells of HeLa, Ca Ski, SiHa, C33-A, C33-A E7, C33A pcDNA, and HT3 cells were seeded in respectively on top of the hard agar. The plate was incubated in a humidified incubator at 37°C with 5% CO<sub>2</sub> for 72 h.

#### 2.2.1 Generation of C33A and HT3 Spheroids Model

##### *Hanging Drop Method*

The generation of C33-A and HT3 spheroids was carried out using the hanging drop method [13]. Approximately 5000 cells were dropped on the inner side of a 100 mm dish lid. Then, 10 ml of 1X PBS was added to the bottom of the dish. The PBS works as a hydration chamber for the cells. A volume of 10 ml of 1X PBS was added to the plate with the lid facing upwards placed on top of the plate. The 100 mm dish was incubated in a humidified incubator at 37°C with 5% CO<sub>2</sub> for 72 h.

### *Ultra-Low Attachment (ULA) 96-Well U Bottom Plate*

Approximately 5000 ( $2.5 \times 10^4$ /ml) C33-A and HT3 cells were seeded respectively in the ultra-low attachment (ULA) 96-well U bottom plate (Corning, USA). The plate was centrifuged at 1200 rpm for two min and later incubated in a humidified incubator at 37°C with 5% CO<sub>2</sub> for 72 h.

### *2.2.2 Embedding Spheroids into the Collagen Matrix*

A prepared mix of 0.2 ml of collagen was added to each well of a 24 well plate. Next, the plate was swirled to ensure the collagen mix was evenly distributed within the well. The plate was then incubated in a humidified incubator at 37°C with 5% CO<sub>2</sub> for 15 min to ensure the collagen solidifies. In the meantime, the spheroids were harvested from the agarose-coated 96-well plate using a 0.2 ml pipette tip and transferred to a 1.5 ml microcentrifuge tube. The harvested spheroids were left to settle by gravity. Once the spheroids settled, the excess media was carefully aspirated from the tube, and 0.3 ml of collagen mix was added into the tube. Then, the 24 well plate was removed from the incubator, and the spheroids in the 0.3 ml collagen matrix were embedded in the collagen matrix-coated plate. The plate was then incubated again in a humidified incubator at 37°C with 5% CO<sub>2</sub> for 30 min to ensure the collagen solidifies. Then, 1 ml of respective media (HeLa, SiHa, C33A, and HT3: DMEM, Ca Ski: RPMI) was added into each well, and the plate was then incubated in a humidified incubator at 37°C with 5% CO<sub>2</sub>. The media was replenished every 72 h for the next ten days of the experiment. Phase-contrast images of the spheroids growth and invasion were taken every 24 h via Zeiss Axio Observer Z1 Microscope under 5X magnification.

### *2.2.3 Live and Dead Staining of the Spheroids*

Media was aspirated carefully from the 24 well plate without disturbing or touching the collagen matrix. The well was washed with 1 ml 1X PBS every 5 minutes three times. The residue of the 1X PBS was aspirated completely. Next, 1 ml of live and dead staining solution was added to each well, followed by incubation in a humidified incubator at 37°C with 5% CO<sub>2</sub> for an hour. Phase-contrast and fluorescent images of the growth and invasion of the spheroids were taken using Zeiss Axio Observer Z1 Microscope under 5X magnification.

## **3 Results and Discussion**

Cancer biology research has significant relationships with the two-dimensional (2D) cell culture model [14]. However, the 2D cell culture lacks in providing the natural 3D environment of cells and therefore will not resemble the functional characteristics of the corresponding tissue *in vivo* accurately [15]. The self-assembled group of cells known as spheroids remains as the foremost cell culture platform. In the 3D cell culture model, the cells adhere to each other in a self-assembly manner rather than adhere to the plastic dish. In recent years, a remarkable approach was taken to establish various 3D cell culture platforms and subsequently implement the 3D cell culture systems for drug discovery, analysis of cancer cell biology, and stem cell along with other cell-based studies [10]. Numerous methods are available for spheroids generation from single suspensions cells. The methods include hanging drop or liquid overlay approach, spinner flasks methods, carboxymethyl cellulose technique and gyratory rotation systems [16]. In recent years, several novel single-use products that are available for high-throughput spheroids production. Although various and new inverted methods are available for the spheroid generation, all the technologies are based on the basic anchorage-independent approach [17]. The fundamental requirement in the spheroids generation prevents the cells from attaching to the culture substratum [18] to enhance cell-cell adhesion resulting in a well-defined spherical structure [17].

The commonly used method is the liquid overly method, a 96-well plate made to be non-adhesive by coating the plate well with thin films of agarose, hydrophobic polymers, including poly (2-hydroxyethyl methacrylate) (PHEMA) or poly-N-p-vinyl benzyl-D-lactonamide [18]. In this experiment, agarose was

used as a coating agent to prevent cell adhesion in the 96-wells plates. The liquid overlay non-adhesive surface prevents cellular adhesion allowing the cells to aggregate upon the surface's meniscus [18]. The scaffold plays the role of a temporary structure that holds the spheroid and mimics the architecture of the tumor microenvironment [18]. This method is simple, labor-intensive, and high biological reproducibility of the spheroids due to a specific number of suspended cells assembled to form a single spheroid.

### ***3.1 Generation of Spheroids from HeLa, Caski, SiHa, C33-A, C33-A-E7, C33-A pcDNA, and HT3 Cells***

HeLa and CaSki cells formed compact spheroids compared to SiHa, which formed flat spheroids meanwhile, C33-A formed loose aggregates within 72 h, respectively. The experiment was repeated with SiHa and C33-A cells by generating spheroids using the liquid overlay method, incubating the cells for 7 days to achieve tight spheroids formation. As the study's objective, the HeLa and CaSki spheroid models were established while SiHa formed flat spheroids structure.

The C33A-E7 incorporated cervical cancer cell line was used to elucidate whether the E7 oncoprotein plays a role in forming the cervical cancer spheroids. C33-A pcDNA used vector control for the C33-E7 cells. Unfortunately, the C33A-E7 and the C33-A pcDNA cells formed loose aggregates, which enable us to know that E7 viral oncoprotein does not contribute to the spheroid formation of the HPV negative cervical cell lines. To compare the non-HPV cell line phenotype, another non-HPV cervical cancer cell line, HT3 was used in this study. It was observed that the HPV negative cell lines C33-A and HT3 formed loose aggregates rather than spheroids after 72 h. Our data showed that HT3, C33-A, C33A-E7, and C33-A pcDNA only formed loose aggregates. All the spheroids generated from the HeLa Ca Ski, SiHa, C33-A, C33-A E7, C33A pcDNA, and HT3 loose aggregates show a uniform and highly reproducible from well-to-well, plate-to-plate, yet indicates the biological variance in term of spheroids shape. Within 5000 cells per well, the HeLa cells form the spheroids on the scale >300  $\mu\text{m}$  size while CaSki produces <200  $\mu\text{m}$  in size, SiHa spheroids on the scale >450  $\mu\text{m}$  (Fig. 1).

### ***3.2 Optimization of C33-A and HT3 Cells Spheroid Formation Using the Liquid Overlay, Ultra-Low Attachment Plate, and Hanging Drop Method***

The optimization of C33-A and HT3 spheroids generation was carried out using three different spheroid generation methods. The methods comprising were liquid overlay method, hanging drop, and ultra-low attachment. The hanging drop method is a well-established approach used for spheroid formation. In this study, the suspension droplet containing the cell sediment was applied underside of the petri dish's lid. Upon lid inversion, surface tension is responsible for keeping the drops in place. The microgravity setting inside every drop allows cell concentration resulting in the formation of spheroids in the free liquid-air interface and subsequently spheroid generation in the cell lines [19]. In this study, each drop of 20  $\mu\text{L}$  in the volume containing approximately 5000s cells was held on the cover of the petri dish and incubated for 72 hours in the humidified incubator at 37°C. Fig. 2 shows that the hanging drop method produced similar loose aggregates of C33-A and HT3 cells as the liquid overlay method.

As a consequence of the loose aggregates' formation by the mentioned two methods, optimization was carried out using the third method. The third established method uses ultra-low attachment U- bottom plate, as the polystyrene surface offers low-adhesion properties [17]. This U-bottom plate is a ready-made 96-well format plate where 5000 cells were seeded into each well, and gentle centrifugation was applied. The plate was then incubated 72 h at 37°C with 5% CO<sub>2</sub>. Unfortunately, the U bottom plate also produced loose aggregates of the C33-A and HT3 cells. According to Weiswald et al. [17], not all cell lines were able to generate compact spheroids. The hanging drop method produced similar spheroids as a liquid overlay method while the ultra-low attachment plate generates the C33-A and HT3 loose aggregates closer in contact than the hanging drop and liquid overlay methods.

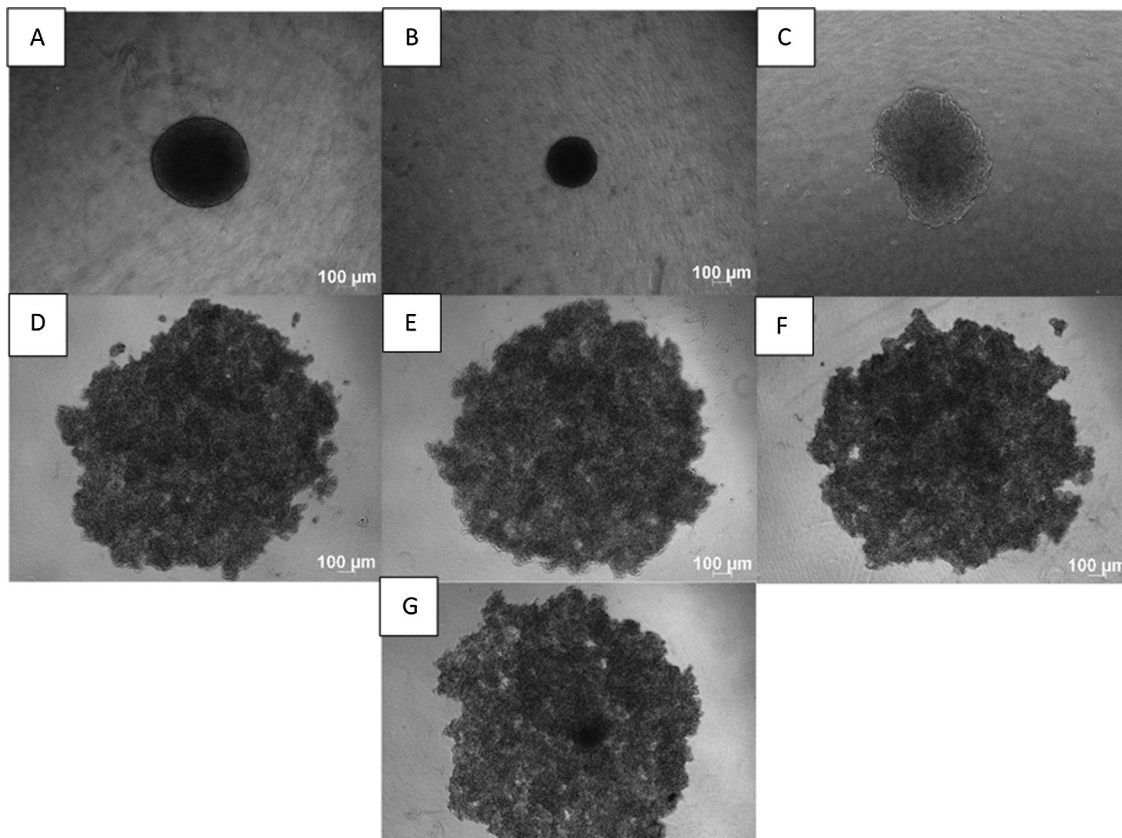


**Figure 1:** 3D Spheroids generated using liquid overlay method. Phase-contrast images of (A) HeLa, (B) CaSki, (C) SiHa (spheroids), (D) C33-A, (E) C33-A E7, (F) C33-A pcDNA, and (G) HT3 loose aggregates cells. Within 5000 cells per well, the HeLa cells form the spheroids on the scale  $>300\ \mu\text{m}$  size while CaSki produces  $<200\ \mu\text{m}$  in size, SiHa spheroids on the scale  $>450\ \mu\text{m}$ . Images were captured under 5X magnification

### 3.3 Formation of C33-A and HT3 Loose Aggregates in the Collagen Matrix

The formed loose aggregates of C33-A and HT3 cells were picked and embedded respectively into the collagen matrix. Random phase-contrast images were taken every 24-h. On Day 10, the experiment was terminated by staining the spheroids using the calcein AM and ethidium homodimer-1. Calcein AM is a commonly used cell-permanent dye for the determination of cell viability in most eukaryotic cells. In analyzing live cells, the calcein AM which by standard do not emit fluorescent, emits a green fluorescent calcein after acetoxymethyl ester hydrolysis by intracellular esterases [20]. Cells appeared as green fluorescence, which indicates they are viable cells. The cell-impermanent viability indicator ethidium homodimer-1 (EthD-1) is a high-affinity nucleic acid stain that is weakly fluorescent until bound to DNA and emits red fluorescence (excitation/emission maxima  $\sim 528/617$ ). Ethidium homodimer-1, which the dead cells picked by integrating into DNA, appeared as red fluorescence dye.

The results indicated that the C33-A and HT3 cells tend to form a spherical structure within the provided collagen matrix on Day 5 (Figs. 3 and 4). Multicellular spheroids were observed throughout the collagen matrix. ECM is known for its role in forming the spheroids within the collagen matrix [21]. There seemed to be a correlation observed with the spheroid formation in the hepatoma cells [13]. The interaction between spheroid cells with neighboring cells and extracellular matrix resulted in their unique

formation of the 3D organization. Here, bovine collagen I was utilized as collagen is the major component of the human ECM.

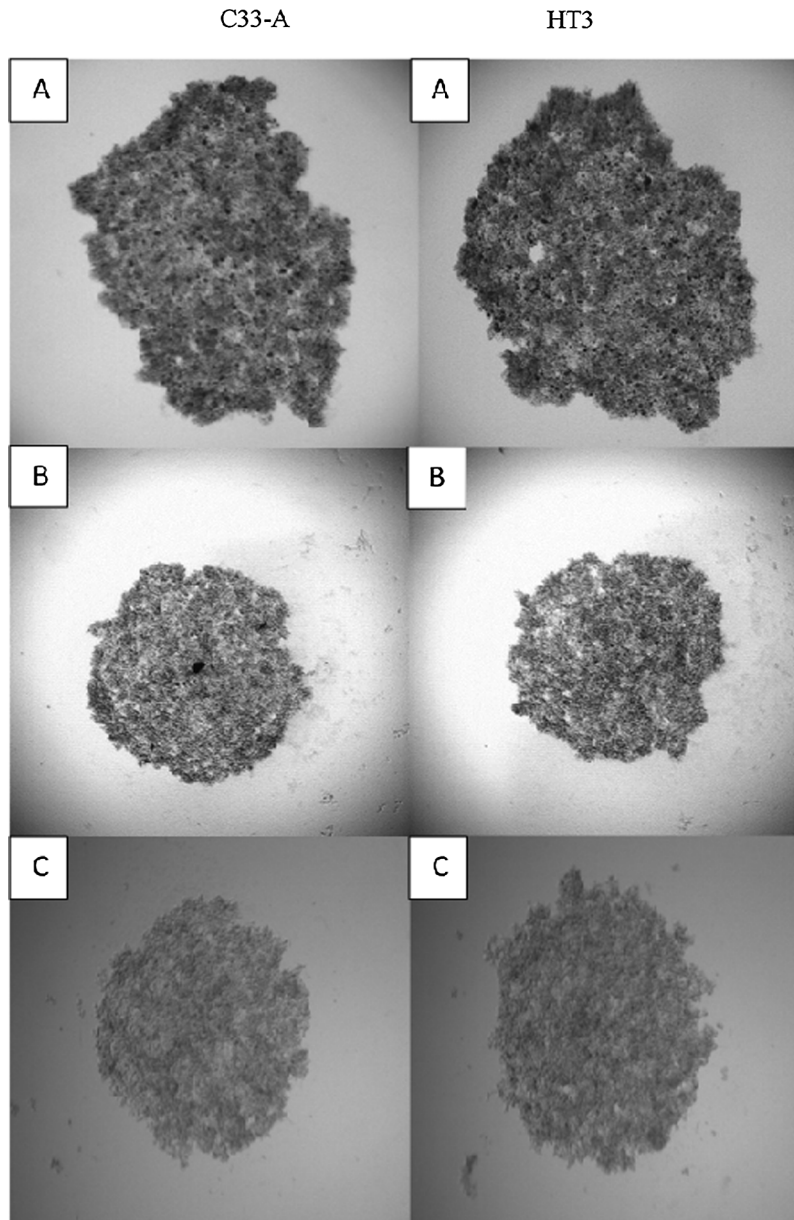


**Figure 2:** Optimization of the C33-A and HT3 cells spheroids formation using three different methods. Method A: liquid overlay method, Method B: ultra-low attachment plate, Method C: hanging drop method. Phase-contrast images of C33-A loose aggregates cells. A and B images were captured under 5X magnification, while image C was captured under 4X magnification. Scale: 100  $\mu$ m

At the molecular level, the molecules which are responsible for spheroids formation remain obscure. Several studies have acknowledged the significance of integrin and cadherins in the formation of spheroid [13,22]. According to Lin et al., the hepatoma spheroids formation involves three stages [13]. The first step involves rapid aggregations of the single cells in the culture medium assisted by the long-chain ECM

fibers with multiple arginyl-glycyl-aspartic acid (RGD) motifs for the cell-surface integrin-binding site [18]. As a second step, up-regulated cadherin expression due to the delay stage of cell aggregation. Lastly, the compact spheroid can be formed as a result of the strong hemophilic binding of cadherin-cadherin between two cells, which enables strong adhesion of the cell [16,18].

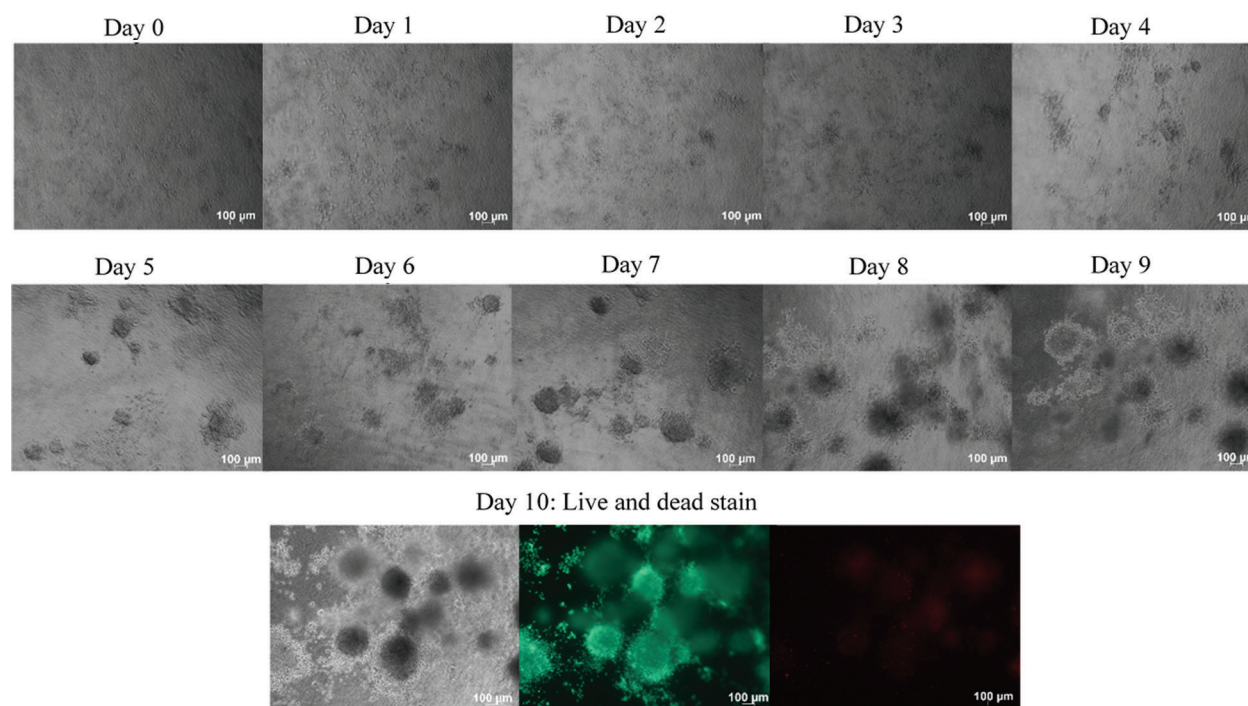


**Figure 3:** C33-A loose aggregates were embedded into the collagen matrix. C33-A loose aggregates were generated using the liquid overlay method and were dispersed into the collagen matrix. Phase-contrast random images of embedded C33-A loose aggregates images were taken every 24 h using Axioz observer, Carl Zeiss, under 5x magnification. C33-A cells formed spheroids when a suitable microenvironment was provided. On day 10, the spheroids were stained with calcein AM and ethidium homodimer-1. Calcein AM stained the viable cells as green, while the ethidium homodimer-1 stained the dead cells as red. Size bar: 100 µm

### 3.4 Formation of HeLa Ca Ski and SiHa Spheroids in the Collagen Matrix

Generated HeLa and CaSki spheroids were embedded, respectively, into the collagen matrix to determine its biological behavior within the matrix. Phase-contrast images were taken from Day 0–Day 10 (Fig. 5). Initial findings indicated a remarkable variation in the growth and invasion phenotype between the HeLa and the CaSki spheroids (Figs. 5 and 6). The HeLa spheroids demonstrated growth and gradual invasion into the collagen matrix. The disintegration of the spheroid core was not observed with the HeLa spheroids (Fig. 5). HeLa maintains the core of the spheroids where it can be postulated that the E-cadherin and integrin might have been up-regulated into the HeLa spheroids.

Cadherins, known as the  $\text{Ca}^{2+}$ -dependent transmembrane proteins family, tend to bind to each other by homophilic interactions [22]. In the cadherins family, the E-cadherin has been known to produce strong cell binding and aid in spheroid formation in several cell types. On the other hand, the integrins, a large family protein known as the heterodimers of  $\alpha$ - and  $\beta$ -subunits, work as the mediator to cell associate with ECM proteins [23]. The ECM gathers the particular type of cell to form a 3D arrangement to initiate the steps

and allow the heterotypic and ECM interactions. The role of E-cadherin is in maintaining the integrity of tissue while integrin interacts with ECMs and plays a role in the cell's migration and invasion [13].

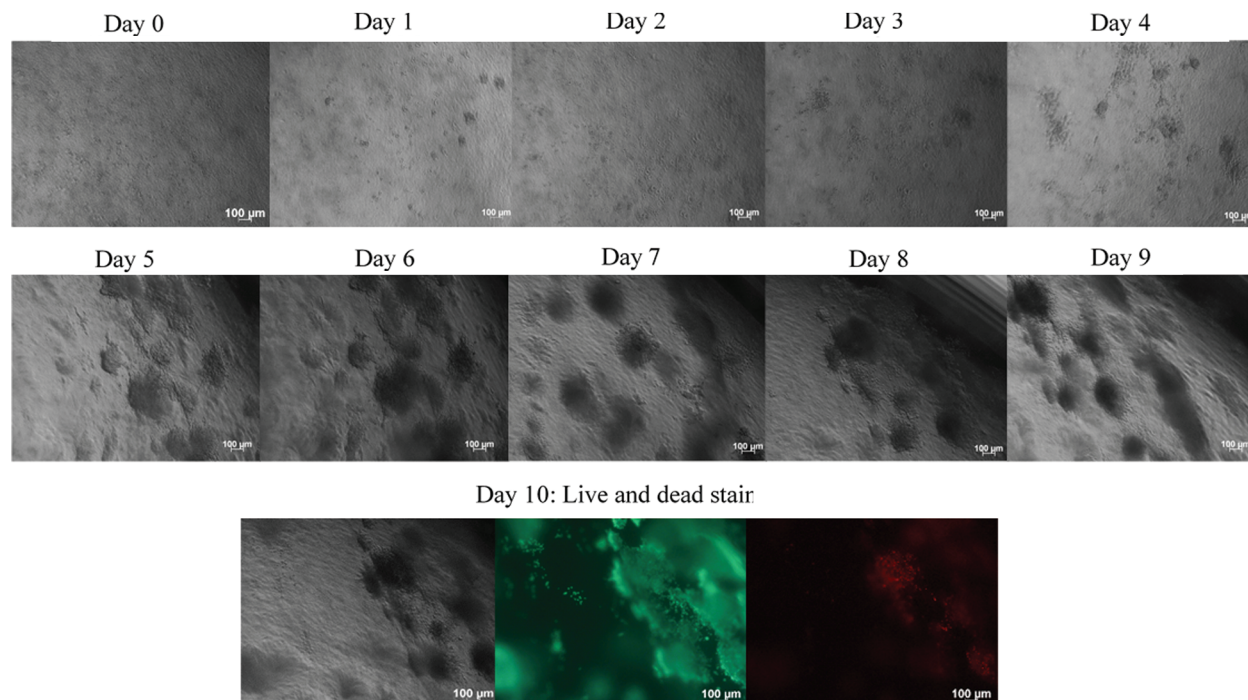


**Figure 4:** HT3 loose aggregates were embedded into the collagen matrix. HT3 loose aggregates were generated using the liquid overlay method and were dispersed into collagen matrix. Phase-contrast images of embedded HT3 loose aggregates images were taken every 24 h using Axioz observer, Carl Zeiss, under 5x magnification. As C33-A cells, HT3 cells also came closer and formed spheroids when a suitable microenvironment was provided. On day ten, the spheroids were stained with calcein AM and Ethidium Homodimer-1. Calcein AM stained the viable cells as green, while the ethidium homodimer-1 stained the dead cells as red. Size bar: 100 µm

The findings from this study indicated that the HeLa spheroid model has a close resemblance to the *in vivo* avascular tumour nodular features and possessed a cellular center (necrotic core). The necrotic core was degenerated, whereas the culture medium contacting outer layer cells (proliferative rim) mimicked the highly proliferative *in vivo* solid tumor cells located near nutrient-rich capillaries. A spheroid consists of proliferating and non-proliferating cells containing both surface exposed and deeply buried cells, well-oxygenated to hypoxic cells [24]. The spheroids core picked the ethidium homodimer-1 while the cells invading into the collagen from the core picked the calcein AM dye, which indicates the cells in the core are partially dead. The invading cells coming out from the core of the spheroids appeared in green, representing viable cells (Fig. 5).

In contrast, Ca Ski spheroids showed an aggressive invasive phenotype (Fig. 6). The phenotype displayed by the Ca Ski spheroids has not been shown or shared by any other spheroids model. The core of the Ca Ski spheroids was completely disintegrated, and the spheroids exhibited an aggressive invasive phenotype into the collagen matrix over 10 days. E-cadherin expression might be low in the CaSki, while up-regulation of integrin can be speculated in the Ca Ski spheroids due to the quick spheroids' disintegration. The disintegration of the spheroids was observed on Day 3 itself, whereas on Day 10 the calcein AM dye was almost everywhere within

the collagen. In other words, the spheroids picked more green dye, indicating more viable cells than the dead cells within the Ca Ski spheroids. Ethidium homodimer dye was not too evident at Ca Ski spheroids due to the disintegration of the spheroids. The aggressive phenotypes displayed by the Ca Ski spheroids indicate the cells were metastatic. Ca Ski's aggressive phenotypic invasion led to a further investigation to compare the spheroid phenotype with other cervical cancer HPV 16 cell line, SiHa.

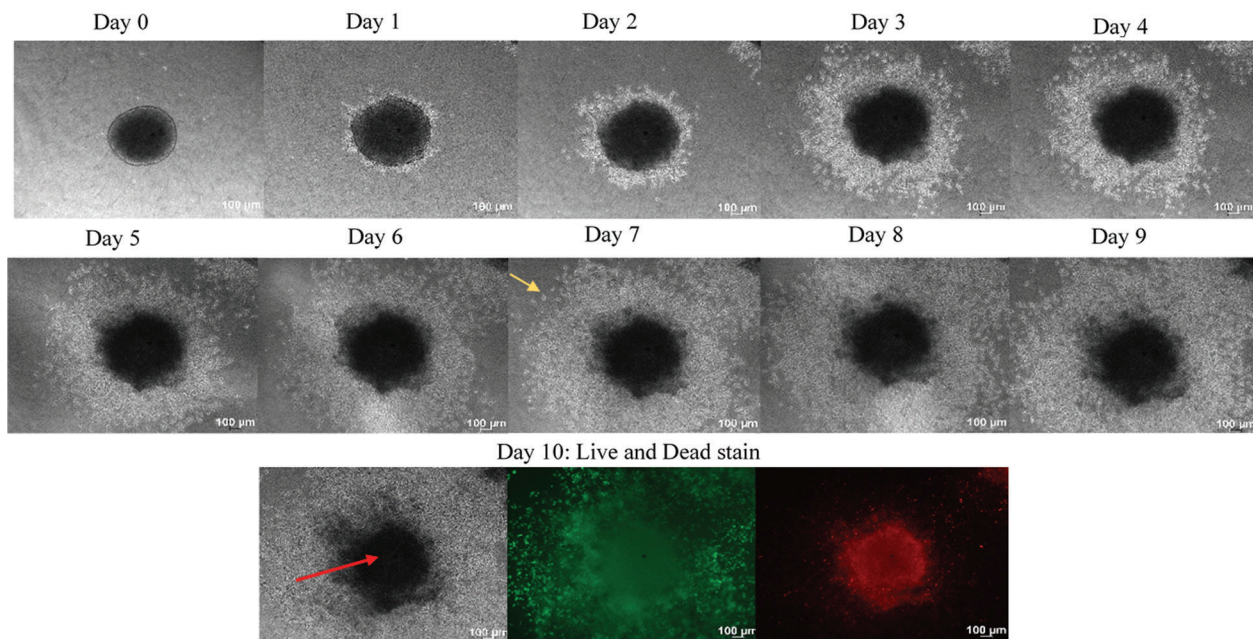


**Figure 5:** Growth and invasion of HeLa spheroids over 10 days. Phase-contrast images of growth and invasion of the spheroids were taken every 24 h using Axio observer, Carl Zeiss, under 5x magnification. The HeLa spheroids show gradual growth and invasion into the collagen matrix over ten days. The red arrows indicate the core, while the yellow arrow indicating the invading cells. The growth shows the increase in the size of the core of the spheroids while the invasion representing the cells invading out from the core of the cells. On day ten, the spheroids were stained with calcein AM and ethidium homodimer –1. Calcein AM stained the viable cells appeared green, while the ethidium homodimer –1 stained the dead cells, which appeared in red. Size bar: 100 µm

The SiHa cells spheroid was generated using the liquid overlay method within 72 h (Fig. 7). Ca Ski formed intact and compact spheroids within 72 h. In contrast, SiHa spheroids were flat and not as compact as Ca Ski or HeLa spheroids. The formed spheroids were embedded into the collagen matrix, and the growth and invasion of the spheroids were measured from Day 0–Day 10. The spheroids were re-structured into a spherical shape on Day 1, indicating the interaction of the cell with the ECM. Contrary to CaSki, the disintegration of the core was not observed in SiHa spheroids. The SiHa spheroids displayed gradual growth and aggressive invasion phenotype into the collagen matrix over 10 days (Fig. 7). We speculate that the HPV 16 copy numbers could contribute to the phenotype. According to the American Tissue Culture Collection datasheet, Ca Ski cells contained 600 copy numbers of HPV16. In comparison, the SiHa consists of 1-2 copy numbers per cell, which may contribute to the aggressive invasion phenotype displayed by the CaSki cells in a three-dimensional system.

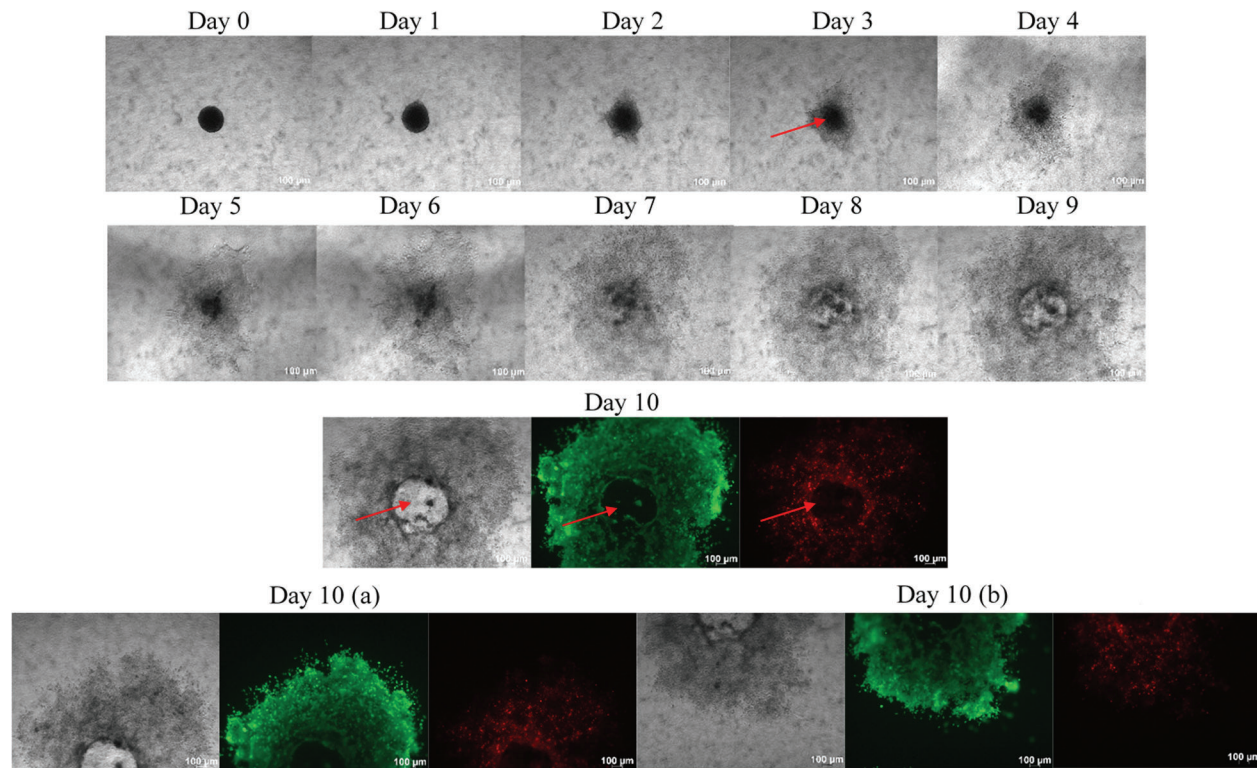


**Figure 6:** Growth and invasion of Ca Ski spheroids over 10 days. Phase contrast images of growth and invasion of the spheroids were taken every 24 h using Axio observer, Carl Zeiss, under 5x magnification. The disintegration of the core was observed at Ca Ski spheroids and aggressive invasion phenotype into the collagen matrix displayed by the Ca Ski spheroids over 10 days. The red arrows indicating fully disintegrated core of spheroids. On day 10, the spheroids were stained with calcein AM and ethidium homodimer –1. Calcein AM stained the viable cells appeared as green while not many dead cells were observed within the Ca Ski spheroids. Due to aggressive invasion, the images were captured as two sessions represent the upper half portion (a) and bottom half portion (b) ensure all the invasion cells were covered within the image. Size bar: 100  $\mu\text{m}$

Kozuka et al., stated that although the copy number per cell was 10-fold higher in CaSki than in SiHa, the E7 mRNA and protein levels per HPV DNA copy were 10 to 20-fold higher in SiHa than in Ca Ski [25]. This is due to the long control regions (LCRs) of SiHa, which indicated a deletion of 38 base pairs that enhanced transcription from P97 detected via a luciferase-expressing plasmid. The up-regulation of E7 appeared to be due to the removal of one of the silencers YY1-binding sites. These findings suggest that mutation affecting YY1-motifs in the LCR is one of the mechanisms enhancing the viral oncogene expression during cancer cell progression [25]. These oncoproteins lead to the induction of genes contributing to cell survival, progression, and potentially the quick invasion behavior of the SiHa.

Spheroids mimic the *in vivo* environment better than standard cell culture techniques combined with the secretion of the necessary growth factors by the cells. Within a 3D structure, cells may demonstrate different functional phenotypes depending on the immediate physical environment. Cells in spheroids more closely resemble the situation *in vivo* with regard to differentiation patterns and spatial cell-cell and extracellular cell matrix (ECM) interactions [13]. The interrelationships of cells with the microenvironment promote the particular cell shape and biological behavior of cells. These spatial and physical aspects in 3D cultures affect the signal transduction from the outside to the inside of cells and ultimately influence gene

expression and cellular behavior [17]. Hence, the 3D system culture offers an efficient *in vitro* platform by mimicking the *in vivo* environments, making it possible to investigate the cellular responses in a setting resembling the actual tumor.

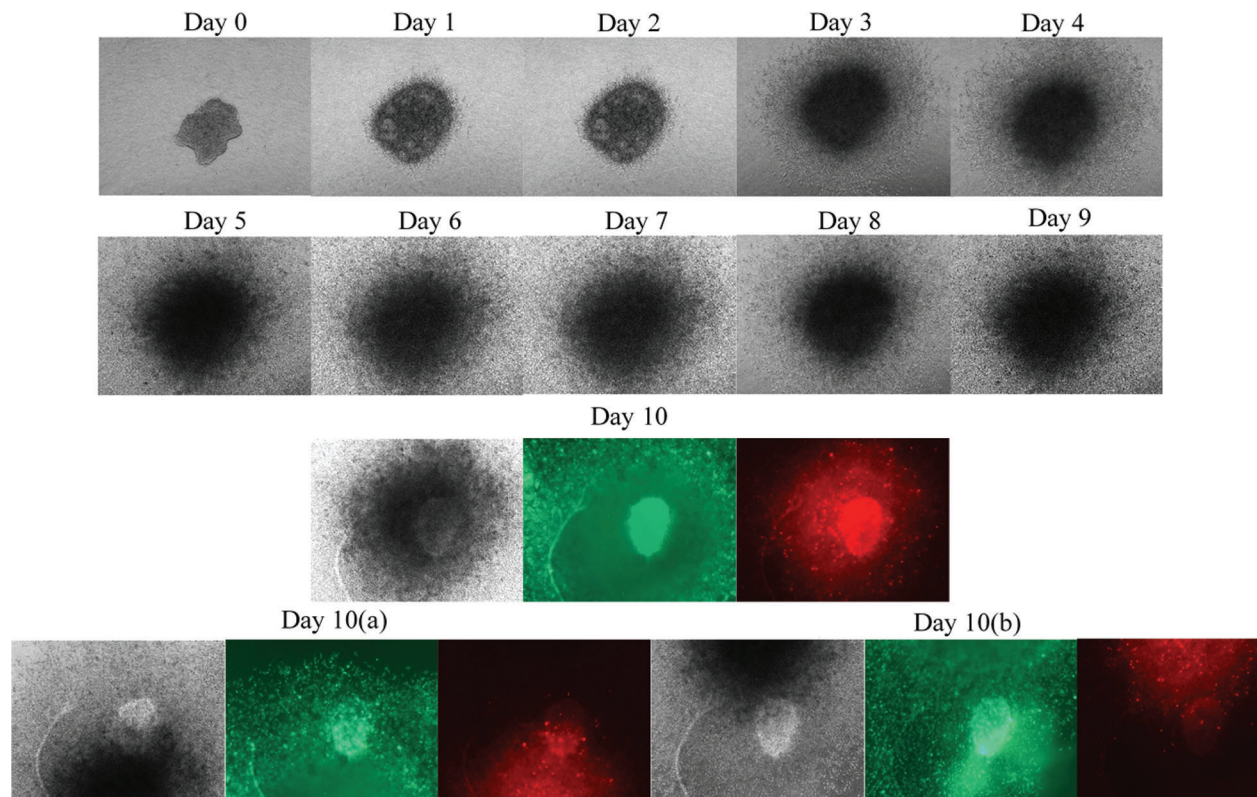


**Figure 7:** Growth and invasion of SiHa spheroids over 10 days. Phase contrast images of growth and invasion of the spheroids were taken every 24 h using Axio observer, Carl Zeiss, under 5x magnification. The disintegration of the core was not observed at SiHa spheroids. The SiHa spheroids displayed gradual growth and invasion phenotype into the collagen matrix over ten days. The core of the spheroids increased in size, and more invading cells were observed by days. At day ten, the spheroids were stained with calcein AM and Ethidium Homodimer –1. Calcein AM stained the viable cells appeared as green, while the Ethidium Homodimer –1 stained the dead cells, which appeared in red. Size bar: 100 $\mu$ m. To cover all the invading cells, images were taken in three angles, covering only the growth in the middle of the core, meanwhile the (a) and (b) pictures at day 10 representing the invading cells

#### 4 Conclusion

The three-dimensional (3D) cell culture provides a fundamental platform for drug discovery and development of treatment for many diseases including, cervical cancer, contributed significantly by the ability of the 3D system to resemble the *in vivo* scenario in aspects of cell morphology and cellular environment. In this study, the 3D spheroids of cervical cancer cell lines, HeLa, Ca Ski, and SiHa were successfully established via the liquid overlay method. Based on the findings, HeLa and CaSki cells were able to form compact spheroids while SiHa cells formed flat spheroid structures. In terms of the biological behavior of the generated cervical cancer spheroids within the matrix, the HeLa spheroids illustrated growth and gradual invasion. In contrast, the Ca Ski spheroids demonstrated an aggressive invasive phenotype that another spheroid model has not shown. The SiHa spheroids displayed

incremental growth and aggressive invasion phenotype into the collagen matrix. In conclusion, the findings of this study would be an initiation point for the preliminary cytotoxic and drug interaction cell-based study for cervical cancer therapeutics specific to the individual HPV infection as the 3D cervical cancer models would provide more reliable data compared to the 2D model.

**Acknowledgement:** We would like to thank Associate Professor Dr. Nikolas Haass (University of Queensland, Australia) for providing the SiHa, C33-A, C33-A E7, C33-A pcDNA and HT3 cell lines.

**Author's Contribution:** K.M.: Methodology, Investigation, Data Analysis and Interpretation and Writing-Original draft preparation. Z.A.A.: Investigation, Data Analysis and Interpretation and Writing-Original draft preparation. S.A.D.: Writing-Review and Editing. S.S.: Writing-Review and Editing. N.M.K.: Supervision and Writing-Review and Editing. V.B.: Conception, Data Analysis and Interpretation, Project administration, Supervision, and Writing-Review and Editing.

**Funding Statement:** The study is part of the research funded by the Ministry of Higher Education Malaysia, Higher Institution Centre of Excellence (HiCoE: 311/CIPPM/4401005), Universiti Sains Malaysia Bridging Grant (304/CIPPM/6316007) and MAKNA Cancer Research Grant (304/CIPPM/650765.M122).

**Conflicts of Interest:** The authors declare that there is no conflict of interest.

## References

- Chen, Z., Schiffman, M., Herrero, R., Desalle, R., Anastos, K. et al. (2011). Evolution and taxonomic classification of human papillomavirus 16 (HPV16)-related variant genomes: HPV31, HPV33, HPV35, HPV52, HPV58 and HPV67. *PLoS One*, 6(5), e20183.
- Global Cancer Observatory (GLOBOCAN) (2020). G.C.O. Summary statistic 2020: Malaysia 2020. <https://gco.iarc.fr/today/data/factsheets/populations/458-malaysia-fact-sheets.pdf>.
- Manan, A. A., Tamin, N. S. I., Abdullah, N. H., Abidin, A. Z., Wahab, M. (2016). *Malaysian national cancer registry (2007–2011)*. National Cancer Institute: Putrajaya: Malaysia.
- Bosch, F. X., Lorincz, A., Muñoz, N., Meijer, C. J., Shah, K. V. (2002). The causal relation between human papillomavirus and cervical cancer. *Journal of Clinical Pathology*, 55(4), 244–265.
- Chow, L. T., Broker, T. R., Steinberg, B. M. (2010). The natural history of human papillomavirus infections of the mucosal epithelia. *Journal of Pathology, Microbiology and Immunology*, 118(6–7), 422–449.
- Fang, Y., Eglén, R. M. (2017). Three-Dimensional cell cultures in drug discovery and development. *SLAS Discovery*, 22(5), 456–472.
- Antoni, D., Burckel, H., Josset, E., Noel, G. (2015). Three-dimensional cell culture: A breakthrough *in vivo*. *International Journal of Molecular Sciences*, 16(3), 5517–5527.
- Eder, J. P., Jr, Supko, J. G., Clark, J. W., Puchalski, T. A., Garcia-Carbonero, R. et al. (2002). Phase I clinical trial of recombinant human endostatin administered as a short intravenous infusion repeated daily. *Journal of Clinical Oncology*, 20(18), 3772–3784.
- Bissell, M. J., Radisky, D. C., Rizki, A., Weaver, V. M., Petersen, O. W. (2002). The organizing principle: microenvironmental influences in the normal and malignant breast. *Differentiation*, 70(9), 537–546.
- Costa, E. C., Moreira, A. F., de Melo-Diogo, D., Gaspar, V. M., Carvalho, M. P. et al. (2016). 3D tumor spheroids: An overview on the tools and techniques used for their analysis. *Biotechnology Advances*, 34(8), 1427–1441.
- Smalley, K. S., Haass, N. K., Brafford, P. A., Lioni, M., Flaherty, K. T. et al. (2006). Multiple signaling pathways must be targeted to overcome drug resistance in cell lines derived from melanoma metastases. *Molecular Cancer Therapeutics*, 5(5), 1136–1144.
- Smalley, K. S., Lioni, M., Noma, K., Haass, N. K., Herlyn, M. (2008). *In vitro* three-dimensional tumor microenvironment models for anticancer drug discovery. *Expert Opinion on Drug Discovery*, 3(1), 1–10.
- Lin, R. Z., Chou, L. F., Chien, C. C., Chang, H. Y. (2006). Dynamic analysis of hepatoma spheroid formation: Roles of E-cadherin and beta1-integrin. *Cell and Tissue Research*, 324(3), 411–422.

14. Stratmann, A. T., Fecher, D., Wangorsch, G., Göttlich, C., Walles, T. et al. (2014). Establishment of a human 3D lung cancer model based on a biological tissue matrix combined with a Boolean in silico model. *Molecular Oncology*, 8(2), 351–365.
15. Edmondson, R., Broglie, J. J., Adcock, A. F., Yang, L. (2014). Three-dimensional cell culture systems and their applications in drug discovery and cell-based biosensors. *Assay and Drug Development Technologies*, 12(4), 207–218.
16. Achilli, T. M., Meyer, J., Morgan, J. R. (2012). Advances in the formation, use and understanding of multi-cellular spheroids. *Expert Opinion on Biological Therapy*, 12(10), 1347–1360.
17. Weiswald, L. B., Bellet, D., Dangles-Marie, V. (2015). Spherical cancer models in tumor biology. *Neoplasia*, 17(1), 1–15.
18. Lin, R. Z., Chang, H. Y. (2008). Recent advances in three-dimensional multicellular spheroid culture for biomedical research. *Biotechnology Journal*, 3(9–10), 1172–1184.
19. Zhang, W., Li, C., Baguley, B. C., Zhou, F., Zhou, W. et al. (2016). Optimization of the formation of embedded multicellular spheroids of MCF-7 cells: How to reliably produce a biomimetic 3D model. *Analytical Biochemistry*, 515, 47–54.
20. Bratosin, D., Mitrofan, L., Paliu, C., Estaquier, J., Montreuil, J. (2005). Novel fluorescence assay using calcein-AM for the determination of human erythrocyte viability and aging. *Cytometry Part A*, 66(1), 78–84.
21. Metzger, W., Rother, S., Pohlemann, T., Möller, S., Schnabelrauch, M. et al. (2017). Evaluation of cell-surface interaction using a 3D spheroid cell culture model on artificial extracellular matrices. *Material Science and Engineering C: Materials for Biological Applications*, 73, 310–318.
22. Angst, B. D., Marcozzi, C., Magee, A. I. (2001). The cadherin superfamily: Diversity in form and function. *Journal of Cell Science*, 114(Pt 4), 629–641.
23. Guo, W., Giancotti, F. G. (2004). Integrin signalling during tumour progression. *Nature Reviews Molecular Cell Biology*, 5(10), 816–826.
24. Yamada, K. M., Cukierman, E. (2007). Modeling tissue morphogenesis and cancer in 3D. *Cell*, 130(4), 601–610.
25. Kozuka, T., Aoki, Y., Nakagawa, K., Ohtomo, K., Yoshikawa, H. et al. (2000). Enhancer-promoter activity of human papillomavirus type 16 long control regions isolated from cell lines SiHa and CaSki and cervical cancer biopsies. *Japanese Journal of Cancer Research*, 91(3), 271–279.